agronomy

MDPI

Article

The Combined Analysis of Transcriptome and Metabolome Provides Insights into Purple Leaves in *Eruca vesicaria* subsp. *sativa*

Dandan Xi [1,†], Xiaofeng Li [1,†], Changwei Zhang [2], Lu Gao [1], Yuying Zhu [1], Shiwei Wei [3], Ying Li [2], Mingmin Jiang [4], Hongfang Zhu [1,*] and Zhaohui Zhang [1,5,*]

1 Shanghai Key Laboratory of Protected Horticultural Technology, Horticultural Research Institute, Zhuanghang Comprehensive Experiment Station, Shanghai Academy of Agricultural Sciences, Shanghai 201403, China
2 State Key Laboratory of Crop Genetics and Germplasm Enhancement, College of Horticulture, Nanjing Agricultural University, Nanjing 210095, China
3 Shanghai Agrobiological Gene Center, Shanghai 201106, China
4 Institute of Vegetable Science, Suzhou Academy of Agricultural Sciences, Suzhou 215155, China
5 Shanghai Runzhuang Agricultural Technology Co., Ltd., Shanghai 201415, China
* Correspondence: zhuhongfang@saas.sh.cn (H.Z.); szyzzh@163.com (Z.Z.)
† These authors contributed equally to this work.

Abstract: Background: Arugula is an essential oil crop of cruciferous species worldwide and serves as a salad vegetable. Purple plant leaves provide nutrients benefiting human beings and are mainly attributed to high anthocyanins. In this study, we collected a purple arugula cultivar with purple leaves and a green arugula with green leaves. The genetic bases and mechanisms underlying purple leaf formation in arugula remain unclear. Therefore, we conducted integrative metabolomics and transcriptomics of two arugula cultivars with different leaf colors. Methods: To study the underlying mechanisms, transcriptomic and metabolomic analyses were carried out. Results: Metabolomic analysis revealed that 84 of 747 metabolites were significantly differentially expressed, comprising 30 depleted and 49 enriched metabolites. Further analysis showed that cyanidin is the main components responsible for the purple color. A total of 144,790 unigenes were obtained by transcriptomic analysis, with 13,204 unigenes differentially expressed, comprising 8120 downregulated and 5084 upregulated unigenes. Seven structural genes, *PAL*, *C4H*, *4CL*, *CHS*, *CCoAOMT*, *LDOX*, and *UFGT*, were identified as candidate genes associated with anthocyanin accumulation through combined analysis of transcriptome and metabolome. Conclusions: Collectively, the differences in the expression levels of *PAL*, *C4H*, *4CL*, *CHS*, *CCoAOMT*, *LDOX*, and *UFGT* might be responsible for purple leaf coloration, providing important data for the discovery of candidate genes and molecular bases controlling the purple leaves in arugula.

Keywords: arugula; green leaf; purple leaf; transcriptome; metabolome

Citation: Xi, D.; Li, X.; Zhang, C.; Gao, L.; Zhu, Y.; Wei, S.; Li, Y.; Jiang, M.; Zhu, H.; Zhang, Z. The Combined Analysis of Transcriptome and Metabolome Provides Insights into Purple Leaves in *Eruca vesicaria* subsp. *sativa*. *Agronomy* **2022**, *12*, 2046. https://doi.org/10.3390/agronomy12092046

Academic Editor: Ainong Shi

Received: 7 July 2022
Accepted: 25 August 2022
Published: 27 August 2022

1. Introduction

Arugula (*Eruca sativa* Mill.), a cruciferous plant, comprises three subspecies: *E. vesicaria* subsps. *Sativa* (*E. Sativa*), *E. vesicaria* subsps. *Vesicaria* (*E. Vesicaria*), and *E. vesicaria* subsps. *Pinatifida* (*E. Pinatifda*) [1]. Arugula grows in drought, dry, and poor soil areas of North America, Asia, and Europe, providing it with outstanding resistance to drought, high salinity, and diseases [2]. Arugula is a diploid (n = 11) and self-incompatible [3], serving as a leafy vegetable with high nutritional value and an oil plant, containing 27.8% oil in seeds [2,4]. Recently, many studies have demonstrated that arugula has potential medicinal properties due to its antioxidant activities [5].

Anthocyanins are phenolic compounds, a group of flavonoids, and responsible for coloring pigments in leaves, flowers, and fruits [6]. More than 635 anthocyanins have been

recognized, comprising six common anthocyanidins: pelargonidin, cyanidin, peonidin, delphinidin, petunidin, and malyidin [6]. Anthocyanins play essential roles in protecting plants against biotic and abiotic stresses, such as low temperature, drought, and insects. Moreover, anthocyanins are also natural edible pigments and have antioxidation and anti-tumor abilities. An apple ERF transcription factor (TF), MdERF38, interacts with MdMYB1 to promote anthocyanin biosynthesis in response to drought stress [7]. Melatonin-induced anthocyanin biosynthesis enhances tolerance to arsenic stress in *Camellia sinensis* L. [8]. Well-established studies have revealed that anthocyanins isolated from purple sweet potato have an effect on colorectal cancer and bladder cancer prevention [9,10]. Anthocyanins extracted from Korean black beans were also reported to enhance ROS levels and antioxidant systems in the amyloid precursor protein/presenilin-1 mouse model of Alzheimer's disease, indicating its potential roles against Alzheimer's disease [11].

Previous studies have characterized the anthocyanin biosynthesis pathway, which is well-understood and conserved in many seed plants [6,12]. Generally, anthocyanins are synthesized from the phenylalanine metabolic pathway. The conversion of phenylalanine to para-coumaroyl-CoA is commonly the first step in the flavonoid biosynthetic route. The anthocyanin synthesis route extends the flavonoid biosynthesis route and begins with the naringenin chalcone produced by *para*-coumaroyl-CoA by chalcone synthase (CHS). Naringenin is quickly synthesized from naringenin chalcone by the action of chalcone-flavanone isomerase (CHI). Naringenin is hydroxylated by flavanone 3-hydroxylase (F3H) and converted into dihydrokaempferol, which is further converted to dihydroquercetin or dihydromyricetin catalyzed by F′3H or F3′5′H, respectively. In the next step, three dihydroflavonols produce the corresponding leucoanthocyanidins by dihydroflavonol-4-reductase (DFR). Leucoanthocyanidins are then converted into the corresponding anthocyanidins (pelargonidin, cyaniding, and delphinidin) through the action of leucoanthocyanidin dioxygenase/anthocyanidin synthase (LDOX/ANS).

During anthocyanin biosynthesis, structural genes and regulatory genes play essential roles. Structural genes encode a series biosynthetic enzymes, comprising early biosynthetic genes and late biosynthetic genes [13]. Regulatory genes usually encode TFs that bind to the promoters of structural genes to regulate their expression. Many studies have demonstrated that the MBW complex involved MYB, bHLH, and WD repeat proteins modulates anthocyanin biosynthesis. PaMYB10, PsMYB58, and MdMYB24 act as positive regulators in anthocyanin biosynthesis, whereas PqMYB4 and PpMYB18 act as negative regulators [14–18].

In the present study, we reported two arugula cultivars, green arugula (GA) and purple arugula (PA), which present with purple leaves and green leaves, respectively. To determine the underlying mechanisms of purple leaf formation, metabolomic and transcriptomic analyses were performed to observe the differences in terms of compounds and gene expression between the two arugula cultivars. Results revealed that 84 metabolites and 8120 unigenes in purple arugula differed from those of green arugula. Among these, five cyanidins accumulated and seven structural genes changed expression levels in purple arugula through combined analyses. Taken together, we believe that the seven structural genes may be responsible for purple leaf formation.

2. Materials and Methods

2.1. Materials

Arugula was purchased from Nantong Shengxiang Agricultural Technology Co., Ltd. (Jiangsu, China) and stored at the Shanghai Agrobiological Gene Center (Shanghai, China). Arugula was planted at the Zhuanghang Comprehensive Experiment Station of Shanghai Academy of Agricultural Sciences. Seeds were cultivated in pots (54 cm × 28 cm tray with 15 × 7 pots, one plant per pot). Growth conditions were set to 25–28 °C and 70% humidity. Pots were watered to keep the soil moist when necessary. The soil used was a 1:1:3 mixture of vermiculite: perlite: nutritive soil. Twenty-day-old seedlings were collected for transcriptomic and metabolomic analyses.

2.2. Metabolite Detection and Data Analysis

Leaves from 20-day-old seedlings were collected for analysis of metabolites. Processing, extraction, and metabolite detection for metabolome were carried out by Wuhan MetWare Biotechnology Co., Ltd. (Wuhan, China). Four biological replicates in each sample were set. The sample extracts were detected by UPLC–ESI-MS/MS (UPLC: SHIMADZU Nexera X2; MS: Applied Biosystems 4500 QTRAP). The mobile phase consisted of solvent A (ultra-pure water with 0.1% formic acid) and solvent B (acetonitrile with 0.1% formic acid). The starting gradient was 95% for solvent A and 5% for solvent B. A linear gradient of 5% for solvent A and 95% for solvent B within 9.0 min was programmed and maintained for one min. Subsequently, the gradient was adjusted to 95% for solvent A and 5% for solvent B within 1.10 min and maintained for 2.9 min. The flow rate was 0.35 mL/min, and the column temperature was 40 °C. The injection volume was 4 μL.

Linear ion trap (LIT) and triple quadrupole (QQQ) scans were acquired on a triple quadrupole-linear ion trap mass spectrometer (API 4500 Q TRAP LC/MS/MS System), which was equipped with an ESI Turbo Ion-Spray interface. Multiple-reaction monitoring (MRM) was used for metabolite quantification using a self-compiled database (Metware database, MWDB). Orthogonal partial least-squares discrimination analysis (OPLS-DA) and variable importance in projection (VIP) were performed to analyze the maximum differences between green arugula and purple arugula. Differential metabolites were determined by VIP > 1.0 and |Log2FC| > = 1. Metabolites were annotated according to the Kyoto Encyclopedia of Genes and Genomes (KEGG) compound database (http://www.kegg.jp/kegg/compound/, accessed on 25 November 2020). Then, annotated metabolites were mapped to the KEGG pathway database (http://www.kegg.jp/kegg/pathway.html, accessed on 25 November 2020).

2.3. Transcriptome Sequencing and De Novo Assembly

Leaves from GA and PA were collected for transcriptome sequencing with three biological replicates of each cultivar. RNA extraction, cDNA library construction, and sequencing were performed by Wuhan MetWare Biotechnology Co., Ltd. (Wuhan, China). Transcriptome sequencing was finished with Illumina HiSeq. After removing the adapter and fragments of less than 20 bp in length, the clean reads were assembled by Trinity in the absence of a reference genome. The sequence assembly quality was evaluated by the number of sequences and total bases, GC percentage, distribution of unigene lengths, mean length, N50, and N90.

To further analyze gene function, the assembled sequences were searched against seven databases as follows: KEGG, NCBI non-redundant database (NR), Swiss-Prot, Trembl, Pfam, eukaryotic Ortholog Groups (KOG) and Gene Ontology (GO). Moreover, gene and transcript expression levels were analyzed by RSEM.

2.4. Differentially Expressed Gene (DEG) Analysis

DEGs were determined by DESeq2 software, with a false-discovery rate (FDR) < 0.05 and | log2FC |> = 1. To further understand the underlying biological functions of DEGs, KEGG and GO enrichment were performed. Moreover, transcription factors (TFs) among the DEGs were predicted using iTAK software.

2.5. Combined Metabolomic and Transcriptomic Analyses

According to the data of metabolite contents and gene expression, combined analyses were performed to integrate metabolomic and transcriptomic data to observe the genes associated with purple coloration. A Pearson correlation coefficient (PCC) > 0.8 was used to determine the correlation between metabolites and genes.

3. Results

3.1. Summary of Metabolomic Analysis

Our study revealed two phenotypic arugula: purple arugula (PA) and green arugula (GA). The leaf veins presented as purple and green in PA and GA, respectively (Figure 1a). To study the different metabolites affecting leaf formation between two cultivars of arugula, metabolomics analysis was performed in two arugula cultivars with four independent biological replicates for each cultivar, resulting in eight samples. We detected a total of 747 metabolites, mainly comprising phenolic acids (115), amino acids and derivatives (97), organic acids (79), nucleotides and derivatives (58), and saccharides and alcohols (49) (Figure 1b). Principal component analysis (PCA) showed that the four biological replicates cluster together, indicating that the detection was reliable (Figure 1c).

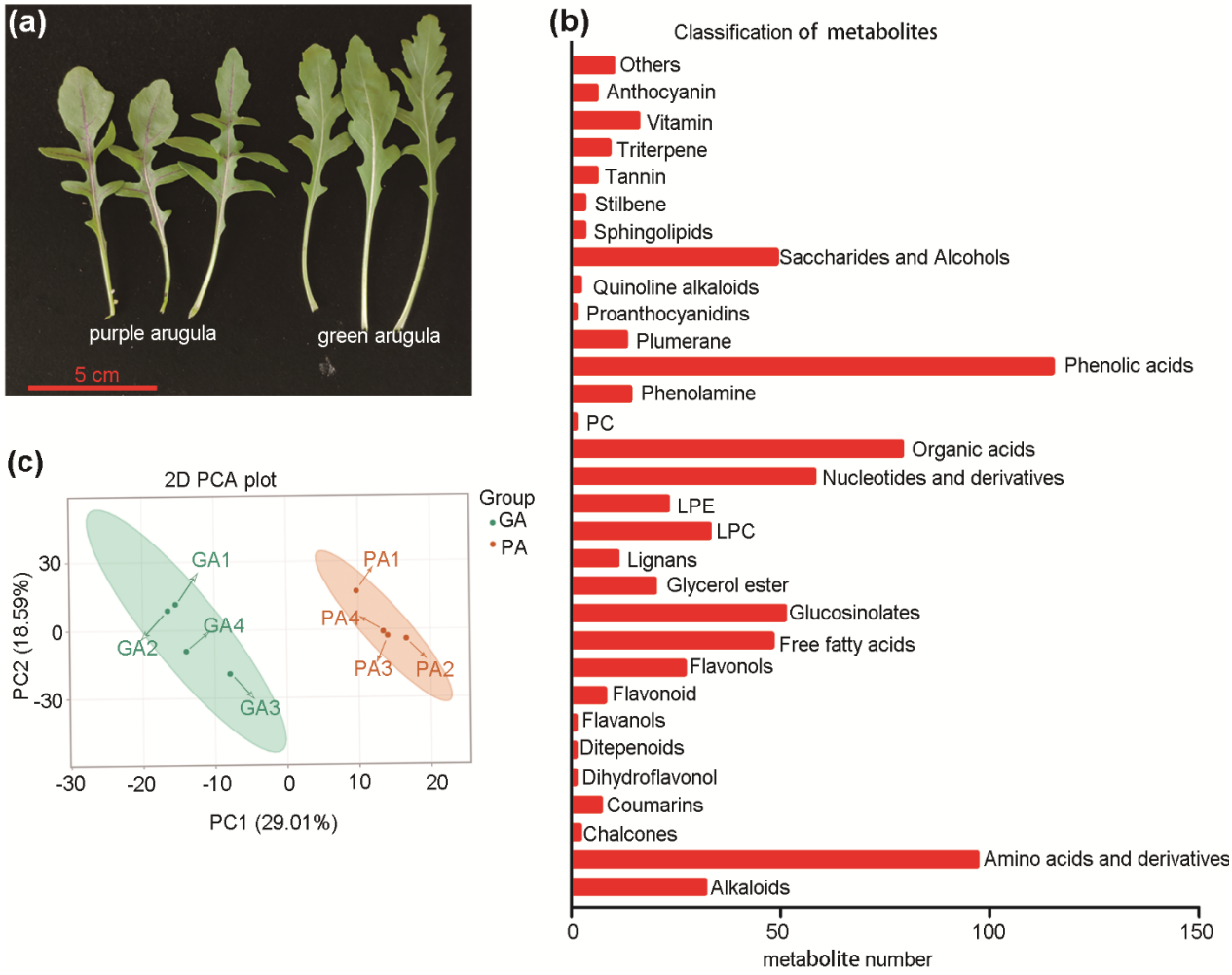

Figure 1. Phenotypes of arugula and overview of metabolome sequencing. (**a**) The phenotypes of two arugula cultivars. Seedlings are 20−days after germination. Red scale bar = 5 cm. PA represents purple arugula, and GA represents green arugula. (**b**) Classification of detected metabolites. PC: phosphatidylcholine; LPE: Lysophosphatidylethanolamine; LPC: lysophosphatidylcholine. (**c**) Principal component analysis (PCA) of the variance-stabilized estimated raw counts of differentially expressed metabolites (DEMs).

3.2. Identification of Differentially Expressed Metabolites

The differentially expressed metabolites (DEMs) were defined by fold change ≥2 or ≤0.5 and variable importance in projection (VIP) ≥1. Among the 747 detected metabolites, we obtained a total of 84 DEMs, including 54 upregulated and 30 downregulated DEMs in purple arugula compared to green arugula (GA vs. PA), including 9 amino acids

and derivatives, 6 phenolamines, 22 phenolic acids, 2 glycerol esters, 2 nucleotides and derivatives, 5 anthocyanins, 10 flavonols, 6 glucosinolates, 2 lignans, 2 tannin, 3 alkaloids, 3 vitamins, 2 coumarins, 5 organic acids, 1 proanthocyanin, 1 plumerane, 1 saccharide and alcohol, 1 flavonoid, and 1 other amino acid (Figure 2a). A total of five anthocyanins were significantly upregulated in PA, including cyaniding-malonylglucoside-sinapoyl-feruloyl-gluside-glucoside (zmzp04816), cyanidin-malonylglucoside-sinapoyl-p-coumaroyl-glucoside-glucoside (zmzp04813), cyanidin-3-O-(6″-O-p-coumaroyl-2‴-O-caffeoyl) sophoroside-5-O-(6⁗-O-malonyl) glucoside (Cwjp002795), and cyanidin-3-O-(6″-O-p-coumaroyl-2‴-O-feruloyl) sophoroside-5-O-(6⁗-O-malonyl) glucoside (zmcp005333), which were among the top four with the largest increase in contents (Figure S1). Furthermore, KEGG enrichment analysis revealed that DEMs were most significantly enriched to tryptophan metabolism, glutathione metabolism, biosynthesis of secondary metabolites, and arginine and proline metabolism (Figure 2b). These data indicate that the purple leaves might be caused by high anthocyanin accumulation in PA.

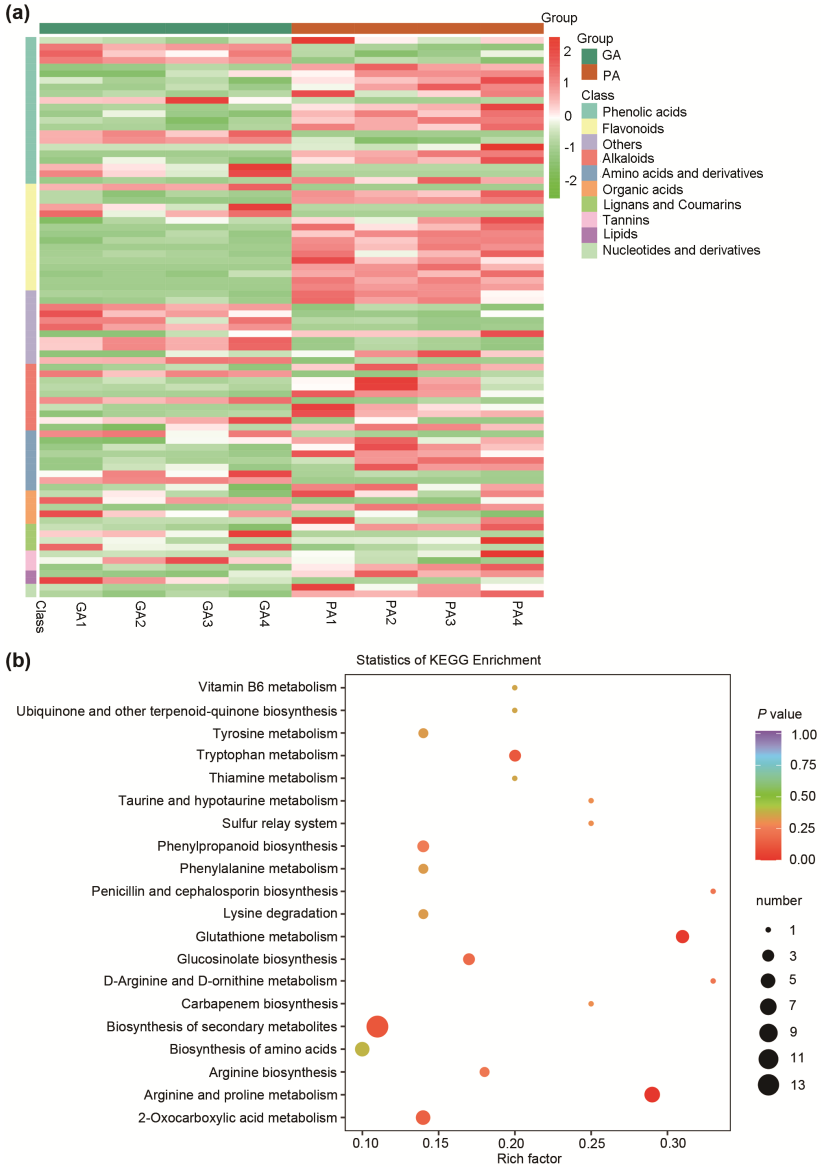

Figure 2. Heat map and KEGG enrichment pathway analyses of DEMs. (**a**) Heatmap diagram of DEMs. Red indicates upregulated metabolites, and green indicates downregulated metabolites. (**b**) Top 30 of KEGG enrichment pathways. Point color indicates $p-$value. Darker shades of red indicate more significant enrichment. Point size indicates gene numbers. Larger points indicate higher gene number.

3.3. Summary of Transcriptomic Analysis

Transcription profiles were also explored with three biological replicates for each cultivar. A total of 38.46 Gb clean data were obtained with 6.41 Gb of each sample. Q30 (%) accounted for more than 94% of each sample. We obtained a total of 144,790 unigenes with an average length of 1233 bp and N50 of 1613 (Table S1). PCA revealed that the GA group showed obvious differences relative to the PA group (Figure 3a). There were 94,829, 128,605, 96,235, 129,054, 78,110, 109,182, and 94,590 unigenes annotated to the KEGG, NR, Swiss-Prot, Trembl, KOG, GO, and Pfam databases, respectively (Figure 3b). Among these annotated unigenes, 130,107 unigenes were annotated in at least one database. With respect to the species distribution of the top BLAST hits in the NR database, 41,974 (32.64%) and 27,167 (21.12%) annotated unigenes matched *Brassica napus* and *Raphanus sativus*, respectively (Figure 3c).

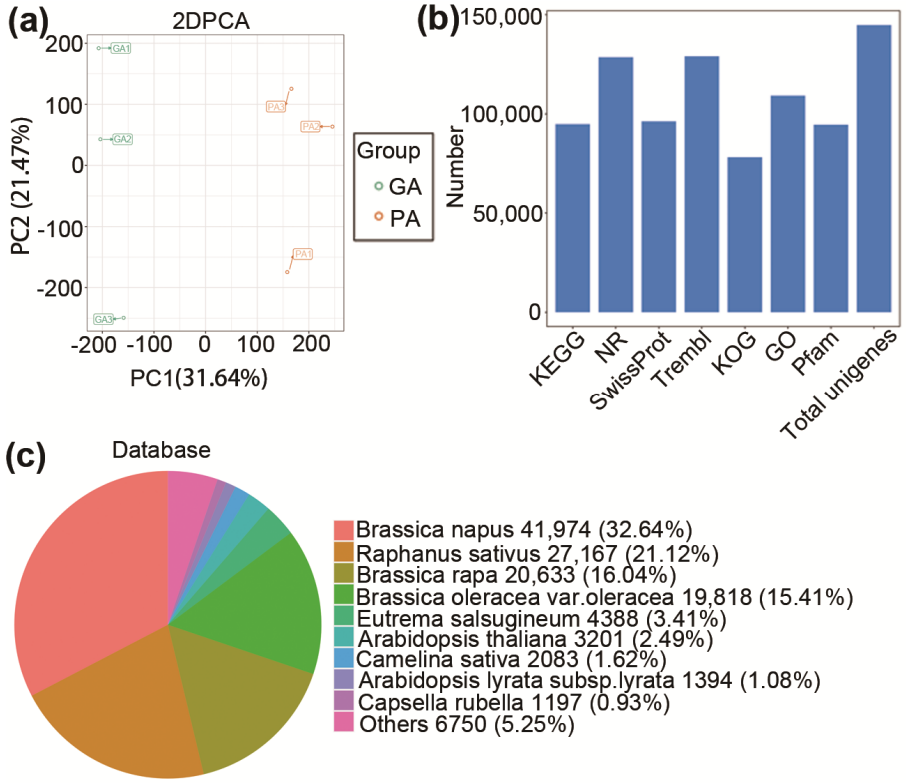

Figure 3. Functional annotation of transcriptome sequencing. (**a**) PCA analysis of the variance-stabilized estimated raw counts of differentially expressed genes (DEGs). (**b**) Functional annotation numbers of unigenes in the KEGG, NR, Swiss-Prot, Trembl, KOG, GO, and Pfam databases. (**c**) Annotated species distribution in the NR database.

3.4. Identification of Differentially Expressed Genes

Differentially expressed genes (DEGs) were defined by |log-2 fold-change > = 1| and a false-discovery rate (FDR) < 0.05. In total, 13,204 DEGs were selected, comprising 8120 downregulated and 5084 upregulated DEGs in GA vs. PA. To determine their potential functions, DEGs were annotated to the GO and KEGG databases. GO enrichment revealed that 9363 DEGs were annotated to the three GO categories: biological process, cellular component, and molecular function. The most significantly enriched GO terms were chaperone-mediated protein folding and 'de novo' protein folding, belonging to biological process; and oxidoreductase activity, acting on NAD (P)H, quinone or similar compound as acceptor, belonging to molecular function (Figure 4a). A total of 5044 DEGs were enriched to 138 KEGG pathways. The most significantly enriched pathways were ubiquinone and other terpenoid-quinone biosynthesis, biosynthesis of secondary metabolites, folate biosynthesis, and biosynthesis of amino acid (Figure 4b). Among these DEGs, 115 unigenes were enriched

to the phenylpropanoid biosynthesis pathway, 25 unigenes to flavonoid biosynthesis, and 5 unigenes to anthocyanin biosynthesis. Moreover, 685 DEGs were predicted to encode TFs, including basic helix–loop–helix (bHLH), C3H, basic leucine zipper (bZIP), AP2/ERF, MYB-related, and NAC, comprising more than 20 members.

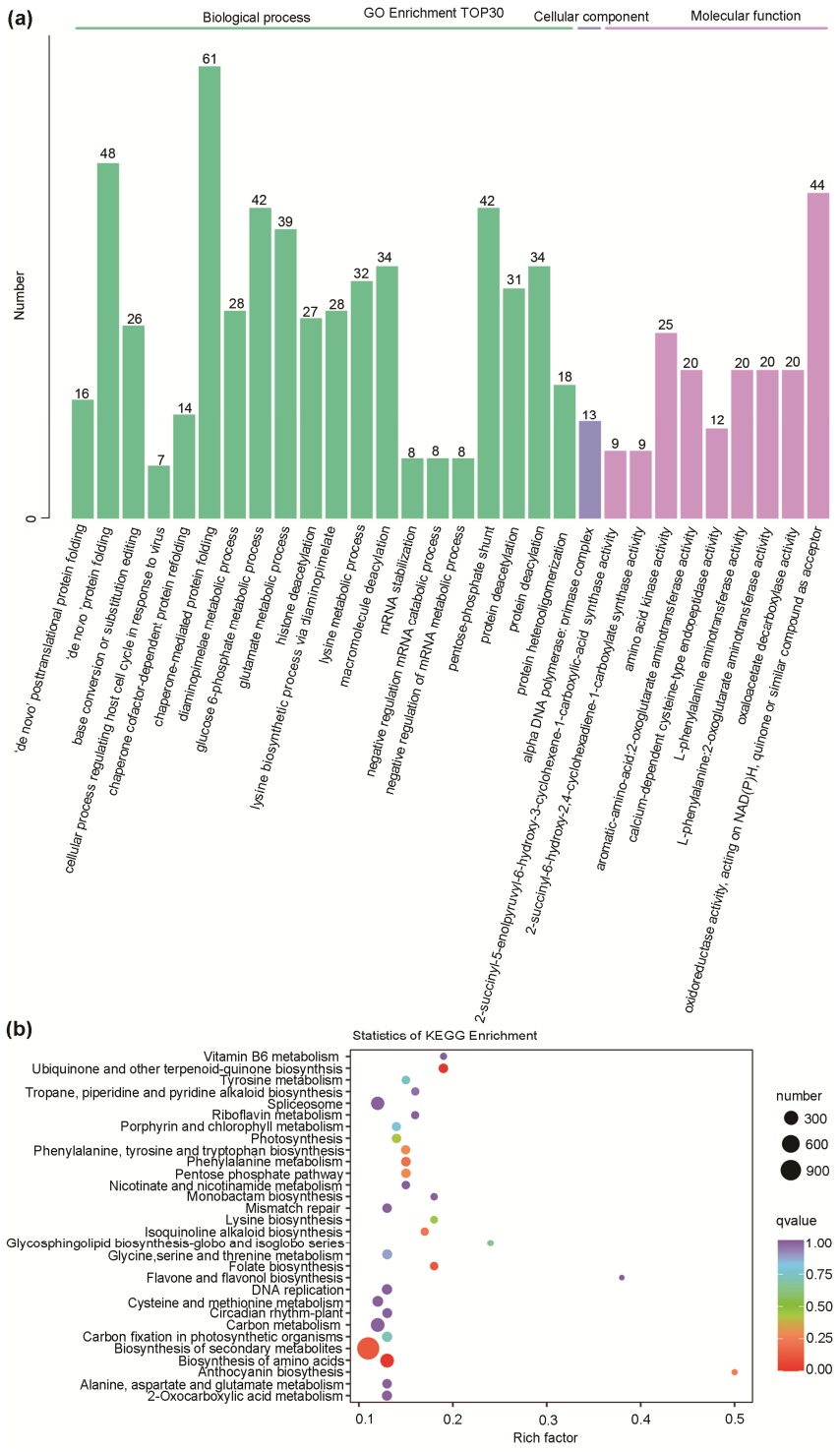

Figure 4. GO and KEGG analyses of differentially expressed genes (DEGs). (**a**) Top 30 of GO enrichment. (**b**) Scatter plot of top 30 KEGG−enriched pathways. The degree of enrichment is identified by rich factor, $q-$value, and the number of DEGs in each pathway.

3.5. Combined Metabolomic and Transcriptomic Analyses

To further understand the relationship between DEGs and DEMs, combined analyses were performed. The nine-quadrant flat revealed that the changes in metabolites and genes were consistent in the third and seventh quadrants, whereas the changes were opposite in the first and ninth quadrants (Figure 5a). A total of 644 DEGs were enriched to the ko00940, ko00941, ko0093, and ko00944 pathways and showed Pearson correlation coefficient (PCC) values ≥ 0.8, with five anthocyanidins, including cyanidin-3-O-(6″-O-p-coumaroyl-2‴-O-feruloyl)sophoroside-5-O-(6⁗-O-malonyl)glucoside, delphinidin 3-glucoside-7,3′-di-(6-(E)-sinapoylglucoside), cyanidin-3-O-(6″-O-p-coumaroyl-2‴-O-caffeoyl) sophoroside-5-O-(6⁗-O-malonyl) glucoside, cyanidin-malonylglucoside-sinapoyl-feruloyl-glucoside-glucoside, and cyanidin-malonylglucoside-sinapoyl-p-coumaroyl-glucoside-glucoside. A total of 22 DEGs encoding seven key enzymes were identified, including twelve phenylalanine ammonia lyase (PAL) genes (cluster-6913.24489, custer-6913.27970, cluster-6913.28356, cluster-6913.38099, cluster-17379.0, cluster-6913.54779, cluster-6913.66205, cluster-2086.1, cluster-6913.82469, cluster-7812.0, cluster-8829.0, and cluster-6913.27971), two 4CL genes (cluster-6913.54468 and cluster-6913.85990), two C4H genes (cluster-6913.85990 and cluster-1892.0), one CHS gene (cluster-6913.56552), three CCoAOMT genes (cluster-6913.34064, cluster-6913.61292, and cluster-3064.0), one LDOX gene (cluster-6913.36682), and one UFGT gene (Cluster-6913.79893) and showed positive correlations with anthocyanidin contents (Figure 5b). These structural genes were significantly upregulated in PA compared with GA (Figure 5b), suggesting their potential roles in anthocyanin biosynthesis and purple leaf formation in arugula.

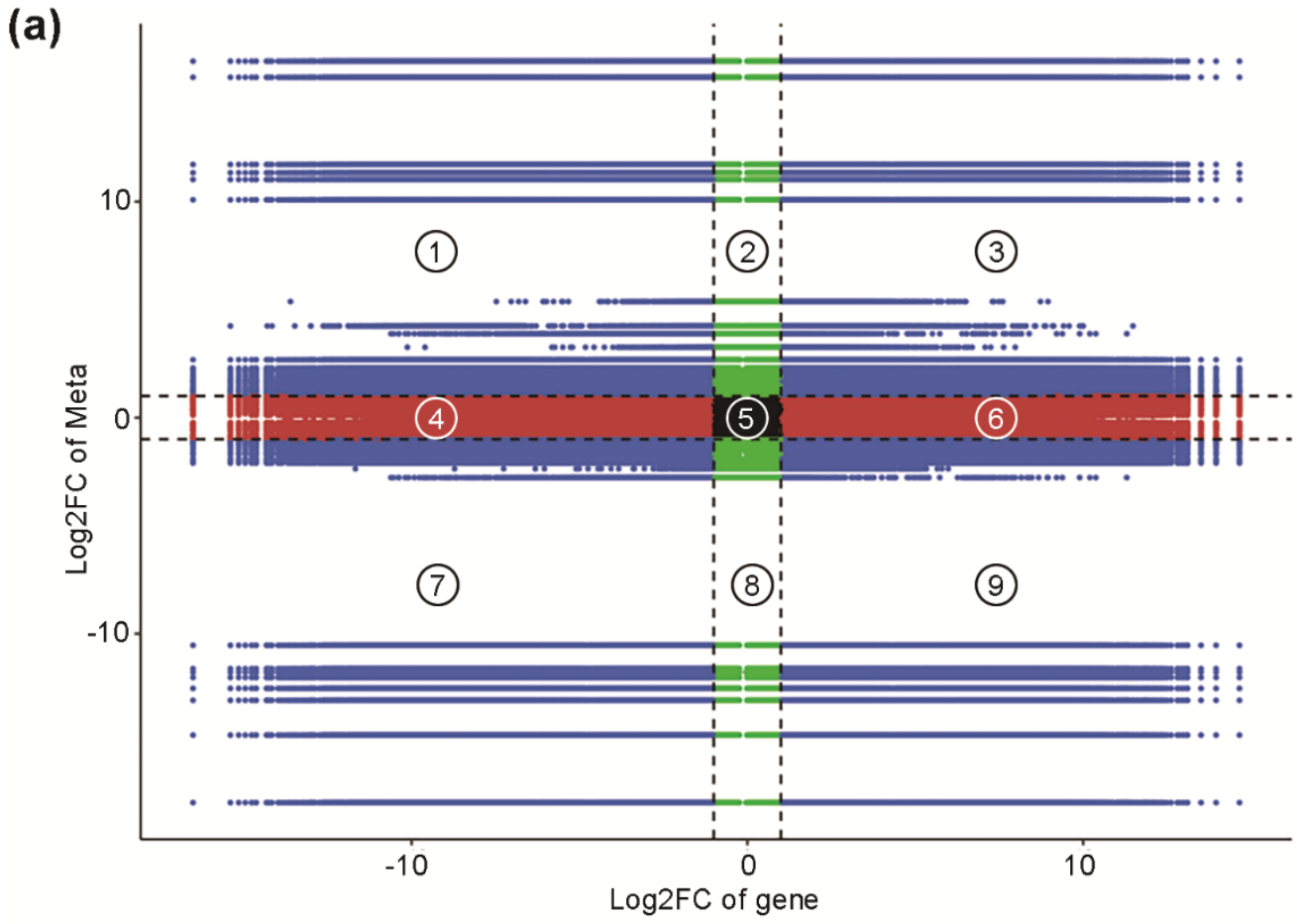

Figure 5. *Cont.*

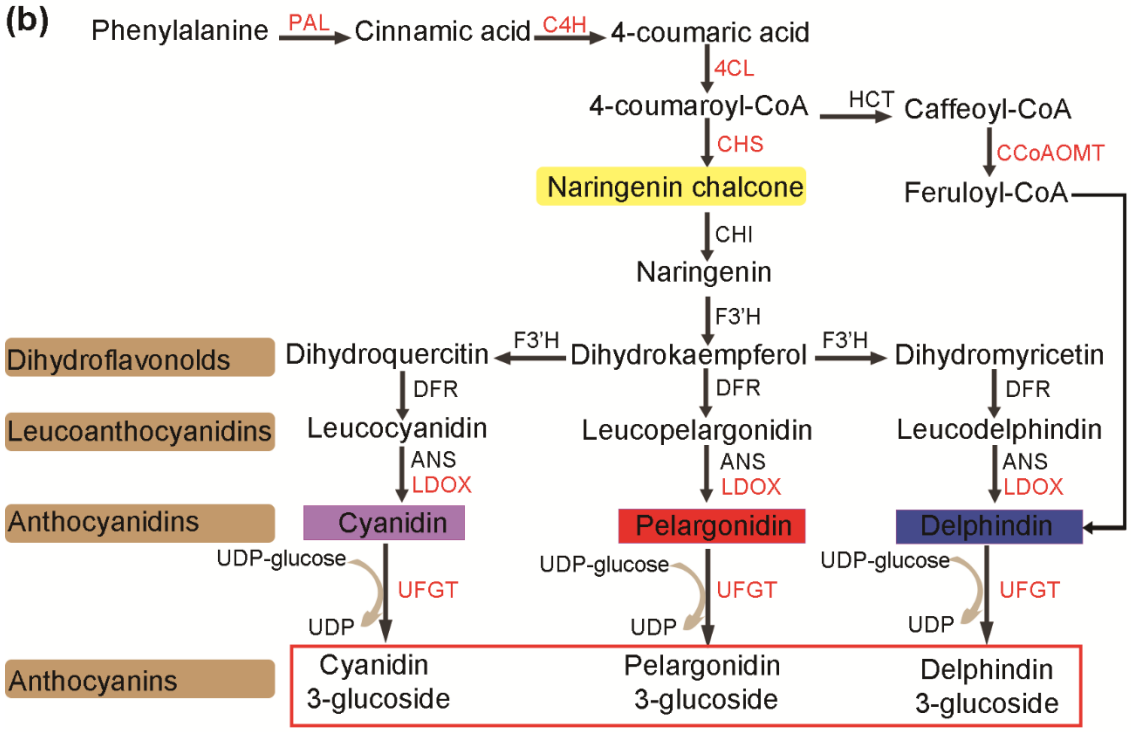

Figure 5. Combined analyses of anthocyanin-related genes and metabolites. (**a**) Nine-quadrant flat. The x-axis represents the log2 ratio of genes. The y-axis represents the log2 ratio of metabolites. Black dotted lines represent different threshold and divide the flat into ①–⑨ quadrants from left to right and from top to bottom. (**b**) Diagram of genes involved in regulating anthocyanins. The red enzymes represent upregulated genes. PAL: phenylalanine ammonia lyase; 4CL: 4-coumarate CoA ligase; C4H: trans-cinnamate 4-monooxygenase; HCT: shikimate O-hydroxycinnamoyltransferase; CHS: chalcone synthase; CHI: chalcone isomerase; F3H: flavanone 3-hydroxylase; F3′H: flavonoid 3′-hydroxylase; DFR: dihydroflavonol 4-reductase; ANS: anthocyanidin synthase; UFGT: anthocyanidin 3-Oglucosyltransferase.

4. Discussion

Arugula is an important oil crop, as well as a popular salad vegetable, with high medicinal values. Previous studies have revealed that three main pigments determine plant colors: chlorophylls, carotenoids, and anthocyanin. Furthermore, anthocyanins are the main factor related to purple color, as confirmed by metabolomic and transcriptomic analyses in many plants, including apple, sugarcane, pear, and ramie [19–22]. In particular, purple coloration in plant leaves was confirmed to be associated with high expression of structural genes and anthocyanin accumulation. In tea, four purple-leaf cultivars presented with high anthocyanin contents compared to green-leaf and yellow-leaf cultivars [23]. Similar results were observed in purple pak choi [24], *Brassica napus* [25], purple sweet potato [26], and birch [27]. These findings revealed the importance of anthocyanins during purple leaf formation and prompted us to propose that the differing leaf colors between two arugula cultivars might be affected by the difference in anthocyanin accumulation.

In the present study, metabolomic analysis confirmed that purple arugula accumulates more flavonoids, phenolic acids, and amino acid and derivatives than green arugula (Figure 2a). In particular, the contents of four cyanidins and one delphinidins, major anthocyanins in plants, significantly were increased in purple arugula relative to green arugula, indicating a relationship with purple leaves (Figure 2a and Figure S1). We further observed that various DEGs changed expression in purple arugula through transcriptomic analysis. Moreover, KEGG analysis showed that most DEGs were enriched during biosynthesis of secondary metabolites (Figure 4b), consistent with the changes in anthocyanin contents between GA and PA. Previous studies identified the structural genes encoding key en-

zymes involved in anthocyanin biosynthesis [12]. We first identified that seven structural genes, *PAL*, *C4H*, *4CL*, *CHS*, *CCoAOMT*, *LDOX*, and *UFGT*, were upregulated in arugula through combined analysis. Their roles in anthocyanin biosynthesis have been verified in various plants, such as apple, rapeseed, and sugarcane [20,21,28]. *PAL* was found to be an early anthocyanin biosynthesis gene, as well as *CHS* and *CHI*. Double-mutant *pal1pal2* exhibited a lack of anthocyanin pigments and yellow leaves [29]. Studies also have revealed that downregulation of *C4H* decreased anthocyanin contents in *Artemisia annua* [30] and the insertion mutant of *LDOX* lacked anthocyanins and caused a "white" pomegranate fruit (*Punica granatum* L.) [31]. An *ufgt3* mutant caused inactive UFGT enzyme and green skin, whereas overexpression of *UFGT3* resulted in anthocyanin accumulation in fruit skin of Japanese apricot (*Prunus mume* Sieb. Et Zucc) [32].Therefore, upregulated structural genes promoted anthocyanin synthesis and maintained anthocyanin stability and solubility, contributing to the purple leaves of PA.

Phenylalanine (Phe) acts as a precursor of many compounds containing flavonoids, isoflavonoids, and anthocyanins. The conversion of Phe to anthocyanins occurs with a series of reactions catalyzed by enzymes, such as PAL, C4H, and 4CL [26]. A previous study demonstrated that Phe was synthesized with two alternative pathways from chorismate, the final product of the shikimate pathway, and required aminotransferases involvement in petunia [33]. Downregulation of a phenylpyruvate aminotransferase gene resulted in reduction of Phe and Phe-derived compounds. In our study, we also observed that a total of 20 unigenes were annotated to the GO term of phenylalanine aminotransferase pathway, implicating active Phe metabolism in arugula (Figure 4a). Furthermore, various unigenes were enriched to the correlated KEGG pathways, phenylalanine metabolism, phenylalanine, tyrosine and tryptophan biosynthesis, and biosynthesis of amino acid (Figure 4b). In addition, biosynthesis pathways of secondary metabolites and anthocyanin, the Phe-derived compounds, were significantly enriched (Figure 4b). These findings are consistent with the expression changes in structural genes and indicate that more Phe might be produced to promote anthocyanin biosynthesis and accumulation in PA.

Many studies have demonstrated that the MBW regulatory model plays crucial roles in anthocyanin biosynthesis. Previous studies revealed AtMYB113/production of anthocyanin pigment 1 (PAP3) and AtMYB114/PAP4 combined with TT8, a bHLH protein, and the WD-repeat protein, TRANSPARENT TESTA GLABRA1 (TTG1), in *Arabidopsis* anthocyanin biosynthesis [34]. MYB3 is highly induced by salt stress and anthocyanin accumulated in *myb3*. Our data include two new genes, cluster-6913.64779 encoding MYB113 and cluster-6913.72222 encoding MYB3. Each of these proteins has a MYB domain at their N terminal. MYB113 and MYB3 show 65.24% and 67.74% similarity with AtMYB113 and AtMYB3, respectively. In the transcription profile, *MYB113* expression was upregulated, and *MYB3* expression was downregulated in PA, indicating that MYB113 was a positive regulator, whereas MYB3 was a negative regulator in anthocyanin biosynthesis in arugula.

A previous study showed that overexpression of *MYC2*, *MYC3*, and *MYC4* promoted anthocyanin accumulation in *Arabidopsis* [35]. MYC3 was found to interact with JASMONATE ZIM-DOMAIN1 (JAZ1) in both yeast two-hybrid and pull-down assays. JAZ1 is a JA signaling repressor and negatively regulates MYB9-dependent anthocyanin biosynthesis through the interaction between MYB9 and TELOMERE-BINDING PROTEIN 1 (TRB1) in apple [36]. Our study revealed an upregulated bHLH gene, *MYC3* (cluster-6913.2187) and six downregulated genes (cluster-6913.27599, cluster-6913.77809, cluster-18276.1, cluster-6913.29549, cluster-7049.0, and cluster-6913.4592) encoding JASMONATE ZIM domain-containing proteins. Therefore, we suspected that MYC3 might interact with JAZ proteins physically to modulate structural gene expression and anthocyanin biosynthesis in arugula.

5. Conclusions

Taken together, the results of our metabolomic and transcriptomic analyses demonstrate that *PAL*, *C4H*, *4CL*, *CCoAOMT*, *LDOX*, *CHS*, and *UFGT* play key roles in anthocyanin biosynthesis in arugula.

Supplementary Materials: The following supporting information can be downloaded at: https://www.mdpi.com/article/10.3390/agronomy12092046/s1, Figure S1: Top 10 upregulated (shown in red bars) and top 10 downregulated (shown in green bars) metabolites in PA compared with GA; Table S1: Summary of transcriptomic data.

Author Contributions: Conceptualization, H.Z. and Z.Z.; validation, D.X., X.L., C.Z., L.G. and Y.Z.; formal analysis, D.X. and L.G.; investigation, X.L., M.J. and Z.Z.; resources, S.W.; supervision, Y.L., H.Z. and Z.Z.; writing—original draft preparation, D.X. and X.L.; writing—review and editing, C.Z., Y.L., H.Z. and Z.Z.; visualization, D.X. and X.L.; project administration, H.Z. and Z.Z.; funding acquisition, M.J. and H.Z.. All authors have read and agreed to the published version of the manuscript.

Funding: This research was funded by the Natural Science Foundation of Jiangsu Province (grant number BK20190168) and the Agriculture Research System of Shanghai, China (grant number 202202).

Institutional Review Board Statement: Not applicable.

Informed Consent Statement: Not applicable.

Data Availability Statement: The transcriptomic sequencing data presented in this study are openly available in NCBI under accession no. SRR15566017-15566020. The associated BioProject is PRJNA756053.

Conflicts of Interest: The authors declare no conflict of interest.

Abbreviations

PA: purple arugula; GA: green arugula; DEM: differentially expressed metabolite; DEG: differentially expressed genes; VIP: variable importance in projection; PCA: Principal component analysis; KEGG: Kyoto Encyclopedia of Genes and Genomes; GO: Gene Ontology; TF: transcription factor; CHS: chalcone synthase; CHI: chalcone-flavanone isomerase; F3H: flavanone 3-hydroxylase; DFR: dihydroflavonol 4-reductase; LDOX: leucoanthocyanidin dioxygenase; ANS: anthocyanidin synthase; PAL: phenylalanine ammonia lyase.

References

1. Warwick, S.I.; Gugel, R.K.; Gómez-Campo, C.; James, T. Genetic variation in Eruca vesicaria (L.) Cav. *Plant Genet. Resour. Charact. Util.* **2007**, *5*, 142–153. [CrossRef]
2. Flanders, A.; Abdulkarim, S.M. The composition of seed and seed oils of taramira. *J. Am. Oil Chem. Soc.* **1985**, *62*, 1134–1135. [CrossRef]
3. Singh, K.; Bhatia, S.; Lakshmikumaran, M. Novel variants of the 5S rRNA genes in Eruca sativa. *Genome* **1994**, *37*, 121–128. [CrossRef] [PubMed]
4. Lidder, S.; Webb, A.J. Vascular effects of dietary nitrate (as found in green leafy vegetables and beetroot) via the nitrate-nitrite-nitric oxide pathway. *Br. J. Clin. Pharmacol.* **2013**, *75*, 677–696. [CrossRef]
5. Keyata, E.O.; Tola, Y.B.; Bultosa, G.; Forsido, S.F. Phytochemical contents, antioxidant activity and functional properties of Raphanus sativus L, Eruca sativa L. and Hibiscus sabdariffa L. growing in Ethiopia. *Heliyon* **2021**, *7*, e5939. [CrossRef]
6. Sunil, L.; Shetty, N.P. Biosynthesi and regulation of anthocyanin pathway genes. *Appl. Microbiol. Biotechnol.* **2022**, *106*, 1783–1798. [CrossRef]
7. An, J.P.; Zhang, X.W.; Bi, S.Q.; You, C.X.; Wang, X.F.; Hao, Y.J. The ERF transcription factor MdERF38 promotes drought stress-induced anthocyanin biosynthesis in apple. *Plant J.* **2019**, *101*, 573–589. [CrossRef]
8. Li, X.; Ahammed, G.J.; Zhang, X.; Zhang, L.; Yan, P.; Zhang, L.; Fu, J.; Han, W. Melatonin-mediated regulation of anthocyanin biosynthesis and antioxidant defense confer tolerance to arsenic stress in *Camellia sinensis* L. *J. Hazard. Mater.* **2021**, *403*, 123922. [CrossRef]
9. Li, W.; Yu, H.; Zhang, X.; Ke, M.; Hong, T. Purple sweet potato anthocyanin exerts antiumor effect in bladder cancer. *Oncol. Rep.* **2018**, *40*, 73–82.
10. Lim, S.; Xu, J.; Kim, J.; Chen, T.; Su, X.; Standard, J.; Carey, E.; Griffin, J.; Herndon, B.; Katz, B.; et al. Role of anthocyanin-enriched purple-fleshed sweet potato p40 in colorectal cancer prevention. *Mol. Nutr. Food Res.* **2013**, *57*, 1908–1917. [CrossRef] [PubMed]
11. Ali, T.; Kim, T.; Rehman, S.U.; Khan, M.S.; Amin, F.U.; Khan, M.; Ikram, M.; Kim, M.O. Natural Dietary Supplementation of Anthocyanins via PI3K/Akt/Nrf2/HO-1 Pathways Mitigate Oxidative Stress, Neurodegeneration, and Memory Impairment in a Mouse Model of Alzheimer's Disease. *Mol. Neurobiol.* **2018**, *55*, 6076–6093. [CrossRef] [PubMed]
12. Alappat, B.; Alappat, J. Anthocyanin pigments: Beyond aesthetics. *Molecules* **2020**, *25*, 5500. [CrossRef] [PubMed]
13. Dubos, C.; Le Gourrierec, J.; Baudry, A.; Huep, G.; Lanet, E.; Debeaujon, I.; Routaboul, J.; Alboresi, A.; Weisshaar, B.; Lepiniec, L. MYBL2 is a new regulator of flavonoid biosynthesis in Arabidopsis thaliana. *Plant J.* **2008**, *55*, 940–953. [CrossRef] [PubMed]

14. Wang, Y.; Liu, W.; Jiang, H.; Mao, Z.; Wang, N.; Jiang, S.; Xu, H.; Yang, G.; Zhang, Z.; Chen, X. The R2R3-MYB transcription factor MdMYB24-like is involved in methyl jasmonate-induced anthocyanin biosynthesis in apple. *Plant Physiol. Biochem.* **2019**, *139*, 273–282. [CrossRef]
15. Xi, W.; Feng, J.; Liu, Y.; Zhang, S.; Zhao, G. The R2R3-MYB transcription factor PaMYB10 is involved in anthocyanin biosynthesis in apricots and determines red blushed skin. *BMC Plant Biol.* **2019**, *19*, 287.
16. Zhou, H.; Lin-Wang, K.; Wang, F.; Espley, R.V.; Ren, F.; Zhao, J.; Ogutu, C.; He, H.; Jiang, Q.; Allan, A.C.; et al. Activator-type R2R3-MYB genes induce a repressor-type R2R3-MYB gene to balance anthocyanin and proanthocyanidin accumulation. *New Phytol.* **2019**, *221*, 1919–1934. [CrossRef]
17. Huo, D.; Liu, X.; Zhang, Y.; Duan, J.; Zhang, Y.; Luo, J. A Novel R2R3-MYB Transcription Factor PqMYB4 Inhibited Anthocyanin Biosynthesis in Paeonia qiui. *Int. J. Mol. Sci.* **2020**, *21*, 5878.
18. Zhang, Y.; Xu, S.; Ma, H.; Duan, X.; Gao, S.; Zhou, X.; Cheng, Y. The R2R3-MYB gene PsMYB58 positively regulates anthocyanin biosynthesis in tree peony flowers. *Plant Physiol. Biochem.* **2021**, *164*, 279–288. [CrossRef]
19. Zhang, Z.; Tian, C.; Zhang, Y.; Li, C.; Li, X.; Yu, Q.; Wang, S.; Wang, X.; Chen, X.; Feng, S. Transcriptomic and metabolomic analysis provides insights into anthocyanin and procyanidin accumulation in pear. *BMC Plant Biol.* **2020**, *20*, 129.
20. Ding, R.; Che, X.; Shen, Z.; Zhang, Y. Metabolome and transcriptome profiling provide insights into green apple peel reveals light- and UV-B-responsive pathway in anthocyanins accumulation. *BMC Plant Biol.* **2021**, *21*, 351.
21. Ni, Y.; Chen, H.; Liu, D.; Zeng, L.; Chen, P.; Liu, C. Discovery of genes involved in anthocyanin biosynthesis from the rind and pith of three sugarcane varieties using integrated metabolic profiling and RNA-seq analysis. *BMC Plant Biol.* **2021**, *21*, 214. [CrossRef] [PubMed]
22. Feng, X.; Gao, G.; Yu, C.; Zhu, A.; Chen, J.; Chen, K.; Wang, X.; Abubakar, A.S.; Chen, P. Transcriptome and metabolome analysis reveals anthocyanin biosynthesis pathway associated with ramie (*Boehmeria nivea* (L.) Gaud.) leaf color formation. *BMC Genom.* **2021**, *22*, 684. [CrossRef] [PubMed]
23. Zhu, M.; Zhou, F.; Ran, L.; Li, Y.; Tan, B.; Wang, K.; Huang, J.; Liu, Z. Metabolic profiling and gene expression analyses of purple-leaf formation in tea cultivars (*Camellia sinensis* var. *sinensis* and var. *assamica*). *Front. Plant Sci.* **2021**, *12*, 606962. [CrossRef]
24. Song, B.; Xu, H.; Chen, L.; Fan, X.; Jing, Z.; Chen, S.; Xu, Z. Study of the relationship between leaf color formation and anthocyanin metabolism among different purple pakchoi lines. *Molecules* **2020**, *25*, 4809. [CrossRef] [PubMed]
25. Li, H.; Du, Y.; Zhang, J.; Feng, H.; Liu, J.; Yang, G.; Zhu, Y. Unraveling the mechanism of purple leaf formation in Brassica napus by integrated metabolome and transcriptome analyses. *Front. Plant Sci.* **2022**, *13*, 945553. [CrossRef] [PubMed]
26. Li, G.; Lin, Z.; Zhang, H.; Liu, Z.; Xu, Y.; Xu, G.; Li, H.; Ji, R.; Luo, W.; Qiu, Y.; et al. Anthocyanin accumulation in the leaves of the purple sweet potato (*Ipomoea batatas* L.) cultivars. *Molecules* **2019**, *24*, 3743. [CrossRef]
27. Lin, L.; Mu, H.; Jiang, J.; Liu, G. Transcriptomic analysis of purple leaf determination in birch. *Gene* **2013**, *526*, 251–258. [CrossRef]
28. Ding, L.; Liu, R.; Li, T.; Li, M.; Liu, X.; Wang, W.; Yu, Y.; Cao, J.; Tan, X. Physiological and comparative transcriptome analyses reveal the mechanisms underlying waterlogging tolerance in a rapeseed anthocyanin-more mutant. *Biotechnol. Biofuels Bioprod.* **2022**, *15*, 55. [CrossRef]
29. Huang, J.; Gu, M.; Lai, Z.; Fan, B.; Shi, K.; Zhou, Y.; Yu, J.; Chen, Z. Functional analysis of the Arabidopsis PAL gene family in plant growth, development, and response to environmental stress. *Plant Physiol.* **2010**, *153*, 1526–1538. [CrossRef]
30. Kumar, R.; Vashisth, D.; Misra, A.; Akhtar, M.Q.; Jalil, S.U.; Shanker, K.; Gupta, M.M.; Rout, P.K.; Gupta, A.K.; Shasany, A.K. RNAi down-regulation of cinnamate-4-hydroxylase increases artemisinin biosynthesis in Artemisia annua. *Sci. Rep.* **2016**, *6*, 26458. [CrossRef]
31. Ben-Simhon, Z.; Judeinstein, S.; Trainin, T.; Harel-Beja, R.; Bar-Ya'Akov, I.; Borochov-Neori, H.; Holland, D. A "white" anthocyanin-less pomegranate (*Punica granatum* L.) caused by an insertion in the coding region of the leucoanthocyanidin dioxygenase (LDOX.; ANS) gene. *PLoS ONE* **2015**, *10*, e142777.
32. Ni, X.; Ni, Z.; Ouma, K.O.; Gao, Z. Mutations in PmUFGT3 contribute to color variation of fruit skin in Japanese apricot (Prunus mume Sieb. et Zucc.). *BMC Plant Biol.* **2022**, *22*, 304. [CrossRef] [PubMed]
33. Yoo, H.; Widhalm, J.R.; Qian, Y.; Maeda, H.; Cooper, B.R.; Jannasch, A.S.; Gonda, I.; Lewinsohn, E.; Rhodes, D.; Dudareva, N. An alternative pathway contributes to phenylalanine biosynthesis in plants via a cytosolic tyrosine: Phenylpyruvate aminotransferase. *Nat. Commun.* **2013**, *4*, 2833.
34. Gonzalez, A.; Zhao, M.; Leavitt, J.M.; Lloyd, A.M. Regulation of the anthocyanin biosynthetic pathway by the TTG1/bHLH/Myb transcriptional complex in Arabidopsis seedlings. *Plant J.* **2008**, *53*, 814–827. [CrossRef] [PubMed]
35. Niu, Y.; Figueroa, P.; Browse, J. Characterization of JAZ-interacting bHLH transcription factors that regulate jasmonate responses in Arabidopsis. *J. Exp. Bot.* **2011**, *62*, 2143–2154. [PubMed]
36. An, J.P.; Xu, R.R.; Liu, X.; Zhang, J.C.; Wang, X.F.; You, C.X.; Hao, Y.J. Jasmonate induces biosynthesis of anthocyanin and proanthocyanidin in apple by mediating the JAZ1–TRB1–MYB9 complex. *Plant J.* **2021**, *106*, 1414–1430. [PubMed]